10.3217/978-3-99161-014-4-039

LESS IS MORE: ADVANCING EEG-BASED ONLINE CONTINUOUS MACHINE ERROR DETECTION WITH THE LIGHTWEIGHT MAX-MIN AMPLITUDE NOISE FILTERING TECHNIQUE

Y. Pan, L. Rabe, M. Klug

Chair of Neuroadaptive Human-Computer Interaction, Brandenburg University of Technology Cottbus-Senftenberg, Cottbus, Germany
Young Investigator Group – Intuitive XR, Brandenburg University of Technology Cottbus-Senftenberg, Cottbus, Germany

E-mail: yanzhao.pan06@gmail.com

ABSTRACT: To apply synchronous laboratory passive brain-computer interface (pBCI) systems to dynamic real-world scenarios, it is essential to develop asynchronous, event-independent pBCIs that can continuously interpret brain activity. Minimizing false alarms (FAs) caused by artifacts in continuous online sessions without compromising the hit rate is one of the primary challenges in EEG-based brain activity classification tasks. To address this challenge, this study introduces the Max-Min Amplitude Noise Filtering (MANF) technique, which is designed to reduce FAs in the online EEG-based machine error detection task. To achieve this, we pre-trained a classifier on labeled data and then tested the performance of the technique on a simulated continuous online classification. The MANF technique, using a predetermined noise threshold, simplifies the noise filtering process by comparing the difference between the maximal and minimal amplitude of incoming EEG data against this threshold, substantially reducing FAs while maintaining high hit rate. This technique outperforms the unfiltered condition and those using the Artifact Subspace Reconstruction technique, achieving an optimal balance between sensitivity and specificity with medium and conservative thresholds. Highlighting the "less is more" principle, the MANF technique proves highly suitable for continuous online pBCI applications. This development contributes to the ongoing efforts in creating more user-friendly and reliable pBCIs for dynamic real-world use.

INTRODUCTION

Passive brain-computer interfaces (pBCIs) derive the output from ongoing brain activity, enriching the human–machine interaction by integrating implicit information on the actual user's intentions and emotional states into technical systems [1]. In recent years, electroencephalogram (EEG)-based pBCIs have been used in various scenarios [2–5], particularly notable in the use of error-related potentials (ErrPs) as implicit feedback. This approach has been validated as feasible in various use cases, e.g. BCI speller [6–8], cursor control [2,9], and improvement of robot control [10–12]. However, most paradigms involved are lab-based and time-locked to specific events. To bridge the gap between synchronous laboratory pBCI systems and dynamic real-world usage, it is essential to develop asynchronous, event-independent pBCIs that can continuously interpret brain activity, ensuring more natural and seamless human-machine interactions. A few studies have investigated continuous, asynchronous error detection [13–15], with the aim of reducing false alarms (FAs) caused by artifacts in continuous online sessions while maintaining precise error detection.

When exploring the real-time classification of EEG signals in dynamic environments or during intense physical activities, artifact interference is a primary obstacle [16,17]. Research in Mobile Brain/Body Imaging [18,19] has highlighted the efficacy of offline artifact correction techniques, such as Independent Component Analysis (ICA), for cleaner signal analysis [20]. Nonetheless, the adaptability of ICA for online application is limited. Novel approaches, including Artifact Subspace Reconstruction (ASR) [21] and Online Recursive ICA [22], show potential in certain online scenarios. However, their performance in continuous, asynchronous online classification, especially considering computational demands, remains unexplored. Therefore, further research is necessary to evaluate the performance of these algorithms or explore new techniques to reduce the effects of artifacts in continuous online application.

This study aims to fill this gap by designing and evaluating a continuous online classification approach that incorporates a novel noise filtering technique. In the context of tactile-based machine error detection, we have implemented a comprehensive methodology that includes feature extraction, class re-balancing, Support Vector Machine (SVM) classifier training, and a simple noise filtering technique. The results indicate that our methodology achieves good performance in the simulation of online continuous classification. Furthermore, through comparative analyses of different noise filtering conditions, we have demonstrated that our simplistic noise filtering technique outperforms both unfiltered conditions and those using the ASR

Published by
Verlag der Technischen Universität Graz

10.3217/978-3-99161-014-4-039

technique. This study highlights the “less is more” principle in controlled continuous online classification scenarios. Therefore, our contributions are twofold: we not only validate the feasibility of a minimalist approach for online machine error detection but also offer insights for future research and applications in EEG-based continuous online classification sessions.

MATERIALS AND METHODS

Materials overview: This study is based on an open-source dataset (https://zenodo.org/records/8345429) [23], which was used for the IJCAI 2023 competition (https://ijcai-23.dfki-bremen.de/competitions/inter-hri/), supported by German Research Center for Artificial Intelligence, Robotics Innovation Center. The dataset contains recordings of the EEG data from eight subjects who were assisted in moving their right arm by an active orthosis. For each participant, 8 labeled single-trial training sets and 2 unlabeled test sets are included. The training sets contain EEG data and all the event markers across the whole experimental sessions, while the test sets contain only continuous EEG data streams and markers indicating the onset of introduced errors.

Participants: The experiment involved 8 healthy right-handed volunteers (4 males and 4 females) with an average age of 21.8 years. Before the experiment, they attended a short session in the lab for an introduction and preliminary tests, which included fitting the orthosis and determining the EEG cap size according to head circumference. All participants were informed of their rights including voluntary withdrawal. The experiment lasted an average of 4.9 hours (SD = 0.6 hours), and participants were remunerated at a rate of 10 euros per hour.

Experimental setup and procedure: Participants were equipped with a 64-channel EEG system and wore an active orthosis on their right arm while holding an air-filled ball in their left hand. The orthosis facilitated the participant's arm movements through a sequence of trials that included both flexion and extension. Certain errors were induced for a short duration of time during these movements. An error was defined as a short-term (250 ms) alteration in the direction of the orthosis's movement. For example, if the orthosis was amid executing a flexion movement, an error would cause a temporary switch to extension before resuming the original flexion path. Similarly, during an extension, it would momentarily change to flexion. The participants' primary task was to identify these errors in the orthosis's operation. The experiment's initial run aimed to establish a baseline with 30 movements without any errors. This was followed by a training session to familiarize the participants with the sensation of the error and the corresponding response — squeezing the ball in the left hand. During the experiment, 6 errors were randomly introduced among 30 movement trials across 10 runs, with the sequence of errors varied in each run. To reduce the artifacts in the data, participants were asked to maintain specific postures and gaze directions. The experiment was designed to elicit a total of 480 error detection responses, calculated from 6 errors in each of the 10 runs, across all 8 participants. The timing of the stimulus onset for the trials without errors was determined by averaging the onset times from the trials that contained errors.

Data acquisition: EEG data collection was performed using the 64-channel LiveAmp system paired with the ActiCap slim electrode setup, adhering to an extended 10-20 layout, both supplied by Brain Products GmbH. The reference and ground electrodes were placed at FCz and AFz, respectively. The impedance for all 64 electrodes was consistently kept below 5 kΩ. Data sampling was at 500 Hz using Brain Products GmbH's Recorder software (version 1.25.0001), which applied hardware filters to limit the data's frequency range to 0.0 Hz to 131.0 Hz. The acquired EEG data was organized in the BrainVision Core Data Format 1.0, comprising three essential files: a binary data file (.eeg), a header file (.vhdr), and a marker file (.vmrk). Within each participant's EEG data folder, the marker files (.vmrk) recorded all critical events during the experiments. Markers for the start of flexion and extension movements were coded as S64 and S32, respectively. Error-free trials are indicated by S48 markers, placed around the calculated mean onset of errors from the trials that contain errors. The introduction of an error in a trial was marked by S96, while the participant's action of squeezing the ball was recorded as an S80 event in the marker file.

Task description and evaluation metrics: For 10 runs from each participant, 8 serve as labeled single-trial training sets for training machine learning models capable of detecting the onset of the deliberately introduced errors in the data, while 2 serve as unlabeled test sets without event markers for model evaluation. During the evaluation phase, a buffer-like sliding window moves through the EEG data along the temporal dimension to simulate continuous online data acquisition. A binary classification of event types (error or non-error) is performed at each position of the sliding window. The predicted error onsets are then compared with true error onsets for evaluation. A predicted error onset that occurs within a 1000 ms window following the true error onset is defined as a hit or true positive. Conversely, any predicted error onset outside this 1000 ms window is defined as a FA or false positive. It is important to note that within the 1000 ms window following a true error onset, multiple error predictions are collectively counted as a single hit, while each FA is included in the cumulative count of FAs. The evaluation metrics consist of the total number of hits in the 2 test sets for all 8 participants (with a maximum of 96), the average number of FAs across the participants, and the average FA rate across the participants. The average FA rate is calculated as the total number of FAs divided by the total number of non-error epochs across the 2 test sessions, averaged across participants.

Preprocessing: For the training sets, EEG data was preprocessed by re-referencing to an average reference

Published by
Verlag der Technischen Universität Graz

10.3217/978-3-99161-014-4-039

and applying a zero-phase, non-causal Hamming windowed-sinc FIR highpass (0.1 Hz passband edge, 0.1 Hz transition bandwidth, 0.05 Hz cutoff frequency (-6db)) and lowpass filter (15 Hz passband edge, 3.75 Hz transition bandwidth, 16.875 Hz cutoff frequency (-6db)) in succession, using the EEGLAB pop_eegfiltnew function. The data was then segmented into epochs of interest, ranging from 100 ms before to 800 ms after the stimulus onset. Baseline correction was applied to each epoch, using the interval from 100 ms before the stimulus to its onset. The error epochs were organized into a [64, 400, 48] matrix indicating the number of channels, time points per epoch, and total error epochs, respectively, derived from 8 training sets per participant, with each set containing 6 error epochs. Similarly, the error-free epochs were organized into a [64, 400, 192] matrix, derived from 8 training sets per participant, with each set containing 24 error-free epochs.

Feature extraction and classifier training: Features were extracted using 50 ms non-overlapping moving windows within the [0-800] ms post-stimulus period across all 64 channels. In each window, the mean value was calculated, resulting in 1024 features per epoch for classification. To address the class imbalance issue, the Synthetic Minority Over-sampling Technique (SMOTE) was applied to enhance the representation of the minority class (error) by generating synthetic samples through interpolation with neighboring instances, thereby equalizing the number of epochs in both classes within the feature matrix [24]. The resulting balanced feature set contained 384 epochs (192 error and 192 non-error epochs), each characterized by a 1024-element feature vector. This feature set served as the input for training the SVM classifier [25]. The SVM model was configured with a linear kernel and a regularization parameter set to 1.0. To validate the model's performance, a 10-fold cross-validation was carried out individually for each participant.

Continuous online classification simulation: During the online classification simulation phase, a buffer-like sliding window moved through the test EEG data along the temporal dimension, simulating the process of continuous real-time data acquisition. Spanning 900 ms, this window covered the same time range used during the offline training phase for feature extraction (including 100 ms baseline range). With a step size of 20 ms, the window continuously "fetched" EEG data, ensuring a seamless and overlapping coverage of the incoming EEG data. The preprocessing approach and feature set chosen for classification in this phase were consistent with those applied in the offline training phase. To reduce the FAs in the continuous classification, we implemented a lightweight noise-filtering technique, termed the "Max-Min Amplitude Noise Filtering (MANF) Technique". The noise level in each window was evaluated and compared to a predetermined threshold. Epochs with a noise level above this threshold were considered "noisy" and directly classified as non-error (0). Finally, the trained

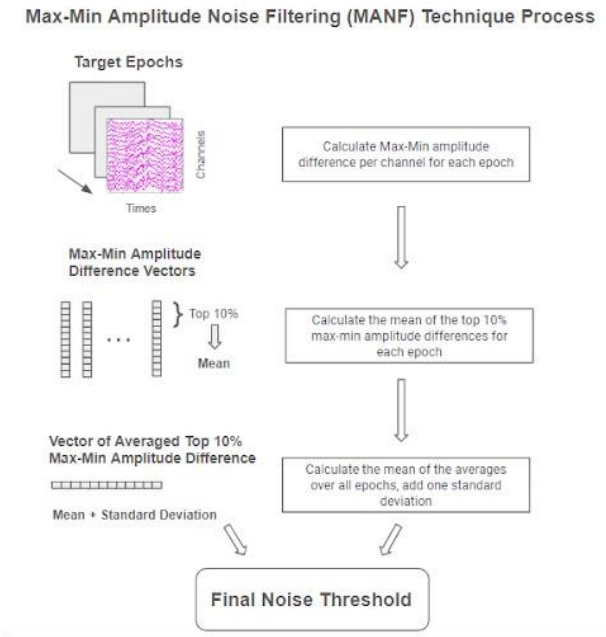

Figure 1: Max-Min Amplitude Noise Filtering (MANF) technique process. This process diagram illustrates the process of determining the noise threshold using target epochs within training sets. First, the max-min amplitude difference within each target epoch is calculated for each channel. Then, the average of the highest 10% of these differences is calculated for each epoch. The final noise threshold is derived by averaging these means over all target epochs and adding a variable number of standard deviations to this average.

SVM classifier continuously provided predictions for each position of the sliding window, where a prediction of 1 indicated the detection of an error, and 0 indicated its absence. Furthermore, we replicated the online simulation using the ASR technique [21] with the 'clean_asr' function in EEGLAB. The evaluation of both the MANF and ASR techniques included three conditions: aggressive, medium, and conservative, each reflecting a different level of noise tolerance. The aggressive strategy used a lower threshold, resulting in more stringent noise filtering, while the conservative strategy adopted a higher threshold, allowing for less stringent filtering. The medium strategy maintained a balance between these two extremes. To implement these strategies, specific hyperparameters were tuned within each technique. For the MANF technique, noise thresholds were set at one, two, and three standard deviations above the mean noise level. For ASR, deviation cutoffs of 5, 20, and 30, relative to calibration data, defined the respective aggressive, medium, and conservative conditions. In addition, a baseline condition without any noise filtering was also evaluated to provide a comparative benchmark.

MANF technique: As shown in Figure 1, a threshold is calculated by examining max-min amplitude differences using the target epochs in the training sets. To this end, first, the max-min amplitude difference

Published by
Verlag der Technischen Universität Graz

10.3217/978-3-99161-014-4-039

Table 1: Online classification simulation results across different noise filtering conditions.

Condition	Total Hits	Average FAs (Mean ± SD)	Average FA Rate (Mean ± SD)
Unfiltered (baseline)	88	957.3 ± 308.6	0.037 ± 0.011
MANF aggressive	80	416.6 ± 158.9	0.016 ± 0.006
MANF medium	86	539.5 ± 186.2	0.021 ± 0.007
MANF conservative	87	620.8 ± 207.5	0.024 ± 0.008
ASR aggressive	26	27.8 ± 22.1	0.001 ± 0.001
ASR medium	81	521.1 ± 192.0	0.020 ± 0.007
ASR conservative	86	653.6 ± 169.5	0.025 ± 0.006

within each target epoch is calculated for each channel. Then, the mean of the top 10% max-min amplitude differences (6 channels/values) is calculated for each target epoch, and last, the mean of those means across all target epochs, plus a variable number of standard deviations, is set as the final noise threshold. In the online simulation phase, epochs that contain mean max-min amplitude differences in their top 10% channels above this threshold are considered "noisy" and excluded from being classified as error epochs.

RESULTS

The pre-trained classifier's performance was evaluated in a 10-fold cross-validation. The average balanced accuracy across all participants was 91.3% ± 4.5% (mean ± SD), which is significantly above the chance level of 0.5 (significance with α = 0.001 would have been reached with 73.68% correct classification, see [26]). The average true positive rate was 84.9% ± 7.8% (mean ± SD), and the average true negative rate was 97.7% ± 1.4% (mean ± SD).

In the continuous online classification simulation phase, 16 test sets, with 2 for each of the 8 participants, were used for online simulation. The average count of non-error epochs across all participants was 26027.0 ± 1733.5 (mean ± SD). The unfiltered condition served as a baseline, yielding the highest total hits and average FAs, as shown in Table 1. When implementing noise filtering using the MANF and ASR techniques with varying hyperparameters, there was a notable decrease in the average FAs. However, this improvement was accompanied by a corresponding reduction in total hits. Figure 2 illustrates the percentage changes in hit rate and average FA rate when applying both noise filtering techniques across three noise tolerance levels. Both techniques substantially reduced the FA rate, with only a relatively minor decrease in the hit rate. The noise filtering strategy that was most aggressive in its approach was the most effective in reducing FAs.

Figure 2: Impact of noise filtering techniques on hit rate and FA rate. This figure compares the percentage changes in hit rate and average FA rate resulting from the application of two noise filtering techniques (MANF and ASR) across three levels of noise tolerance: aggressive, medium, and conservative.

However, it also resulted in the largest decline in hit rate. This was particularly noticeable when using the ASR technique in its aggressive application, where there was a 97.0% reduction in FAs but an unacceptable 70.5% drop in hit rate. The medium and conservative conditions produced a more balanced outcome, with both techniques achieving similar reductions in FAs (43.2% and 34.7% for MANF, and 45.1% and 31.7% for ASR, under medium and conservative conditions, respectively). Notably, the MANF technique outperformed the ASR in preserving the hit rate, showing only a 2.3% reduction compared to 8.0% under the medium condition, and a 1.1% reduction compared to 2.3% under the conservative condition. To demonstrate the process of continuous error prediction in the online simulation, we display the error predictions and true error onsets over time using a test set from one participant as an illustrative example (see Figure 3). This visualization is presented for both the baseline condition and the MANF condition, across three different noise threshold levels.

DISCUSSION

This study investigates the issue of artifact interference in continuous online classification of EEG signals, with a focus on machine error detection. We introduced and evaluated a simple noise filtering technique and found it to be superior to the unfiltered condition and those using the ASR technique in terms of reducing FAs while maintaining the hit rate. Specifically, our noise filtering technique achieved a 43.2% reduction in FA rate with only a 2.3% decrease in hit rate using a medium noise threshold, and a 34.7% reduction in FA rate with a minimal 1.1% decrease in hit rate using a conservative noise threshold. The comparative analysis of different noise filtering conditions highlights an essential consideration in the design of noise filtering strategies: the trade-off between sensitivity and specificity. While aggressive noise filtering effectively minimizes FAs, it may also inadvertently filter out genuine signals, leading to missed detections. Especially when using an

Published by
Verlag der Technischen Universität Graz

10.3217/978-3-99161-014-4-039

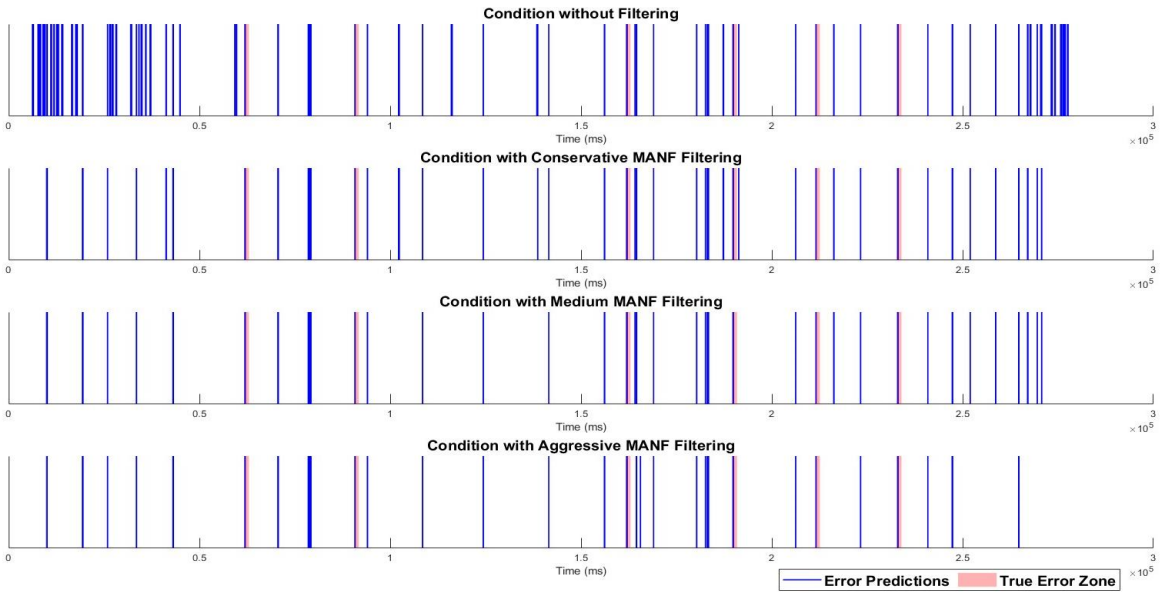

Figure 3: Visualization of continuous error prediction in online simulation. This figure displays the temporal distribution of error predictions (indicated by blue vertical lines) and true error onsets (highlighted with light red shadows) for both the baseline and MANF-filtered conditions across three different noise threshold levels. The data presented here is specific to participant "AQ59D", using test set 6 as an illustrative example.

aggressive cutoff with the ASR technique, this approach tends to remove a significant portion of valuable signal features. As a result, the signals become flattened and lose their distinctive characteristics. Conversely, less stringent filtering preserves more hits but at the risk of higher FA rates. Therefore, for practical applications, it is recommended to use the medium or conservative strategies of the MANF technique. These strategies effectively minimize FAs while preserving a satisfactory hit rate, making them a preferable choice over the ASR technique or no filtering. Besides, the simplicity of the MANF technique offers an additional advantage. This technique simplifies the noise detection process by calculating the difference between the maximum and minimum EEG amplitudes for new incoming data streams in online sessions, and then comparing this calculated difference with a predetermined noise threshold value. This computational efficiency makes the MANF technique particularly suitable for continuous online applications, providing a computationally lightweight and effective solution for enhancing pBCI systems. In essence, this approach perfectly illustrates the "less is more" principle.

The implications of our findings extend beyond the context of tactile-based machine error detection and shed light on the broader domain of asynchronous, continuous online EEG-based classification tasks. The results suggest that the MANF technique shows potential in developing more intuitive and user-friendly pBCI systems, such as assistive devices. By effectively reducing FAs, it promises smoother and more reliable human-machine interactions. However, it is important to note that the MANF technique primarily focuses on excluding noisy epochs rather than correcting artifacts, which might limit its effectiveness in dynamic environments with substantial movement. Advancing artifact correction techniques in such environments is still crucial. Furthermore, the testing phase of our study was conducted through an online simulation. Therefore, future research should evaluate the performance of the MANF technique in real online sessions and across diverse EEG-based applications, especially in complex or unpredictable environments. Additionally, further investigation into the optimization of noise filtering parameters, possibly through machine learning algorithms or adaptive filtering techniques, could yield even more effective and flexible solutions.

CONCLUSION

This study demonstrates that the MANF noise filtering technique can substantially reduce FAs while maintaining a high hit rate, outperforming both unfiltered conditions and those using the ASR technique in continuous online EEG signal classification. This approach, emphasizing the "less can be more" principle, offers a computationally efficient solution for enhancing pBCI systems, particularly in applications requiring continuous, real-time interaction. Our work contributes to the field by validating a minimalist yet effective strategy for online machine error detection and providing a foundation for future research in EEG-based continuous online classification. Looking forward, it is essential to explore the generalizability of the MANF technique in dynamic environments and further refine noise filtering parameters to broaden its applicability and effectiveness.

Published by
Verlag der Technischen Universität Graz

10.3217/978-3-99161-014-4-039

REFERENCES

[1] T. O. Zander and C. Kothe, “Towards passive brain-computer interfaces: applying brain-computer interface technology to human-machine systems in general,” J. Neural Eng., vol. 8, no. 2, p. 025005, Apr. 2011.
[2] T. O. Zander, L. R. Krol, N. P. Birbaumer, and K. Gramann, “Neuroadaptive technology enables implicit cursor control based on medial prefrontal cortex activity,” Proc. Natl. Acad. Sci. U. S. A., vol. 113, no. 52, pp. 14898–14903, Dec. 2016.
[3] F. Dehais et al., “Monitoring Pilot’s Mental Workload Using ERPs and Spectral Power with a Six-Dry-Electrode EEG System in Real Flight Conditions,” Sensors , vol. 19, no. 6, Mar. 2019, doi: 10.3390/s19061324.
[4] A. Mora-Sánchez, A.-A. Pulini, A. Gaume, G. Dreyfus, and F.-B. Vialatte, “A brain-computer interface for the continuous, real-time monitoring of working memory load in real-world environments,” Cogn. Neurodyn., vol. 14, no. 3, pp. 301–321, Jun. 2020.
[5] T. O. Zander and S. Jatzev, “Context-aware brain–computer interfaces: exploring the information space of user, technical system and environment,” J. Neural Eng., vol. 9, no. 1, p. 016003, Dec. 2011.
[6] M. Spüler, M. Bensch, S. Kleih, W. Rosenstiel, M. Bogdan, and A. Kübler, “Online use of error-related potentials in healthy users and people with severe motor impairment increases performance of a P300-BCI,” Clin. Neurophysiol., vol. 123, no. 7, pp. 1328–1337, Jul. 2012.
[7] M. Bevilacqua, S. Perdikis, and J. D. R. Millan, “On Error-Related Potentials During Sensorimotor-Based Brain-Computer Interface: Explorations With a Pseudo-Online Brain-Controlled Speller,” IEEE Open J Eng Med Biol, vol. 1, pp. 17–22, Feb. 2020.
[8] P. Margaux, M. Emmanuel, D. Sébastien, B. Olivier, and M. Jérémie, “Objective and Subjective Evaluation of Online Error Correction during P300-Based Spelling,” Advances in Human-Computer Interaction, vol. 2012, Dec. 2012, doi: 10.1155/2012/578295.
[9] O. E. Krigolson, C. B. Holroyd, G. Van Gyn, and M. Heath, “Electroencephalographic correlates of target and outcome errors,” Exp. Brain Res., vol. 190, no. 4, pp. 401–411, Oct. 2008.
[10] S. K. Kim, E. A. Kirchner, A. Stefes, and F. Kirchner, “Intrinsic interactive reinforcement learning – Using error-related potentials for real world human-robot interaction,” Sci. Rep., vol. 7, no. 1, pp. 1–16, Dec. 2017.
[11] S. K. Ehrlich and G. Cheng, “A Feasibility Study for Validating Robot Actions Using EEG-Based Error-Related Potentials,” International Journal of Social Robotics, vol. 11, no. 2, pp. 271–283, Apr. 2019.
[12] A. F. Salazar-Gomez, J. DelPreto, S. Gil, and D. Rus, “Correcting robot mistakes in real time using EEG signals,” in 2017 IEEE International Conference on Robotics and Automation (ICRA), unknown, May 2017, pp. 6570–6577.
[13] C. Lopes-Dias et al., “Online asynchronous detection of error-related potentials in participants with a spinal cord injury using a generic classifier,” J. Neural Eng., vol. 18, no. 4, p. 046022, Mar. 2021.
[14] J. Omedes, I. Iturrate, and L. Montesano, “Asynchronous detection of error potentials,” in Proceedings of the 6th Brain-Computer Interface Conference 2014, 2014.
[15] M. Spüler and C. Niethammer, “Error-related potentials during continuous feedback: using EEG to detect errors of different type and severity,” Front. Hum. Neurosci., vol. 9, p. 155, Mar. 2015.
[16] A. Tandle, N. Jog, P. D’cunha, and M. Chheta, “Classification of artefacts in EEG signal recordings and EOG artefact removal using EOG subtraction,” Commun. Appl. Electron., vol. 4, no. 1, pp. 12–19, Jan. 2016.
[17] D. Gorjan, K. Gramann, K. De Pauw, and U. Marusic, “Removal of movement-induced EEG artifacts: current state of the art and guidelines,” J. Neural Eng., vol. 19, no. 1, Feb. 2022, doi: 10.1088/1741-2552/ac542c.
[18] S. Makeig, K. Gramann, T.-P. Jung, T. J. Sejnowski, and H. Poizner, “Linking brain, mind and behavior,” Int. J. Psychophysiol., vol. 73, no. 2, pp. 95–100, Aug. 2009.
[19] K. Gramann et al., “Cognition in action: imaging brain/body dynamics in mobile humans,” Rev. Neurosci., vol. 22, no. 6, pp. 593–608, Nov. 2011.
[20] T. P. Jung et al., “Removing electroencephalographic artifacts by blind source separation,” Psychophysiology, vol. 37, no. 2, pp. 163–178, Mar. 2000.
[21] C. A. E. Kothe and T.-P. Jung, “Artifact removal techniques with signal reconstruction,” 20160113587:A1, Apr. 28, 2016 Accessed: Mar. 06, 2024. [Online]. Available: https://patentimages.storage.googleapis.com/c3/6b/dc/7dadfae33c0062/US20160113587A1.pdf
[22] S.-H. Hsu, T. R. Mullen, T.-P. Jung, and G. Cauwenberghs, “Real-Time Adaptive EEG Source Separation Using Online Recursive Independent Component Analysis,” IEEE Trans. Neural Syst. Rehabil. Eng., vol. 24, no. 3, pp. 309–319, Mar. 2016.
[23] N. Kueper et al., “EEG and EMG dataset for the detection of errors introduced by an active orthosis device,” arXiv [cs.HC], May 19, 2023. [Online]. Available: http://arxiv.org/abs/2305.11996
[24] N. V. Chawla, K. W. Bowyer, L. O. Hall, and W. P. Kegelmeyer, “SMOTE: Synthetic Minority Over-sampling Technique,” jair, vol. 16, pp. 321–357, Jun. 2002.
[25] C. Cortes and V. Vapnik, “Support-vector networks,” Mach. Learn., vol. 20, no. 3, pp. 273–297, Sep. 1995.
[26] G. R. Mueller-Putz, R. Scherer, C. Brunner, R. Leeb, and G. Pfurtscheller, “Better than Random? A closer look on BCI results,” Int. J. Bioelectromagn., vol. 10, no. 1, pp. 52–55, Jan. 2008.

Published by
Verlag der Technischen Universität Graz